Electronic Supplementary Material (ESI) for Sustainable Energy & Fuels.

Supporting Information

Bias-free photoelectrochemical H_2O_2 production with a solar-to-fuel conversion efficiency of 2.33%

Dan Zhu, Chao Feng, Zeyu Fan, Beibei Zhang, Xin Luo and Yanbo Li*

Institute of Fundamental and Frontier Sciences, University of Electronic Science and Technology of China, Chengdu 610054, China.

*E-mail: yanboli@uestc.edu.cn

Experimental details

Materials. Ordered mesoporous carbon (CMK-3), anion exchange ionomer (Fumion FAA-3), and carbon cloth (CeTech W1S1011) were purchased from SCI Materials Hub. Magnesium oxide (MgO, 99.99% in purity) and tantalum oxide (Ta_2O_5, 99.99% in purity) evaporation sources and niobium (Nb) foil (0.1 mm in thickness, 99.99% in purity) were purchased from ZhongNuo Advanced Material (Beijing) Technology. H_3BO_3 (99.5% in purity), $NiSO_4 \cdot 6H_2O$ (99.99% in purity), $Co(NO_3)_2 \cdot 6H_2O$ (99.99% in purity), $FeSO_4 \cdot 7H_2O$ (99.95% in purity), KOH (95% in purity) were purchased from Aladdin Chemicals. H_2O_2 (30% in purity) aqueous solution was purchased from Chengdu Kelong Chemicals. All the chemicals were used as-received without purification.

Preparation of Mg:Ta_3N_5/NiCoFe-B_i photoanode. The gradient Mg-doped Ta_3N_5 thin films were prepared by dual-source electron beam evaporation and thermal nitridation following our previously reported precudure[1]. The Nb foils (1×1 cm^2 or 3.33×3 cm^2 in size) and quartz glass (1×1 cm^2 in size) were cleaned by ultrasonication in precision detergent (Alconox), deionized water, acetone, and isopropanol, each for 15 min. The Nb foils were then etched with a mixed solution (HF: HNO_3: H_2O = 1:2:7) for 2 min, rinsed with deionized water, and dried under a stream of nitrogen. Gradient Mg-doped tantalum oxide (Mg:TaO_x) thin films were deposited on the Nb foil and quartz glass substrates by dual-source electron beam evaporation (Angstrom Engineering AMOD) using MgO and Ta_2O_5 as the evaporation sources. The deposition rate of Ta_2O_5 was fixed at 5 A/s, while the deposition rate of MgO varied linearly from 0.9 to 0.4 A/s. The thickness of the deposited Mg:TaO_x film was approximately 680 nm. The prepared Mg:TaO_x precursor films were then heated in a horizontal quartz tube furnace at 1273 K for 6 h under 200 sccm NH_3 flow to obtain gradient Mg:Ta_3N_5 films. The back side of the Nb substrate was attached to a copper wire by soldering with indium and then encapsulated with epoxy resin (Araldite). The electrodes were etched with a mixture of HF:HNO_3:H_2O (1:2:7 in v/v) for 20 s and rinsed with deionized water

to prepare a fresh surface for co-catalyst modification. NiCoFe-B_i co-catalyst was deposited on the gradient Mg:Ta_3N_5 photoanode by photo-assisted electrodeposition. The deposition solution was a 0.25 M potassium borate ($K_2B_4O_7 \cdot 4H_2O$) buffer (pH 10) containing 2 mM $NiSO_4$, 0.5mM $Co(NO_3)_2$ and 0.8 mM $FeSO_4$. Photo-assisted electrodeposition was carried out in the solution under Ar purge and magnetic stirring at a constant current density of 30 μA/cm^2 for 10 min under the illumination of AM 1.5G simulated sunlight. After deposition, the electrodes were rinsed with deionized water.

Preparation of CC/CMK-3 cathode. The CC/CMK-3 cathode was prepared by drop-casting CMK-3 ink onto the carbon cloth (CC). The CMK-3 ink was prepared by adding 3.4 mg of CMK-3 catalyst into a mixture of 0.41 ml of deionized water, 1.63 ml of isopropanol, and 0.36 ml of Fumion FAA-3, followed by ultrasonication for 2 h. The carbon cloth was cut into 1 × 1 cm^2 or 6 × 6 cm^2 pieces and placed on a hotplate heated at 90 °C. Then, the CMK-3 ink was drop-casted onto the carbon cloth at a loading amount of 60 μL/cm^2 (i.e., 0.085 mg/cm^2 of CMK-3 catalyst) and left on the hotplate for 15 min. Carbon paper/CMK-3 cathode loaded with the same amount of CAM 1.5G simulated sunlight illumination different amounts of CMK-3 catalyst were prepared in a similar way.

Photoelectrochemical measurements of the Mg:Ta_3N_5 photoanode. The PEC properties of the Mg:Ta_3N_5 photoanode for water oxidation were measured on a potentiostat (BioLogic SP-200) in three-electrode configuration using a Pt counter electrode and a Hg/HgO reference electrode. The Pt cathode chamber and the photoanode chamber were separated using a Nafion 117 membrane. A class AAA solar simulator (SAN-EI ELECTRIC, XES-40S3-TT) was used as the light source, and the irradiance was adjusted to 100 mW cm^{-2} using a certified reference cell (Konica-Minolta AK-200). The temperature of the electrolyte (1 M KOH, pH 13.6) was maintained at 283 K using a constant temperature water bath during the PEC test. Linear sweep voltammograms (J-V curves) were recorded under an anodic scan at a rate of 10

mV s^{-1} under simulated sunlight. Chronoamperometry test was conducted at an applied potential of 1 V versus RHE under simulated sunlight.

Photoluminescence measurement of Mg:Ta_3N_5 film. The low-temperature PL spectrum of the Mg:Ta_3N_5 film deposited on a quartz glass substrate was measured using a Picoquant FluoTime 300 system under the excitation of a 510 nm pico-second laser. The temperature of the sample was cooled using a closed-cycle He cryostat (ARS DE-202) to ~10 K.

Calibration of H_2O_2 concentrations in 1 M KOH electrolyte. The amount of H_2O_2 in the 1 M KOH electrolyte was determined by colorimetry of the color changes from Fe^{2+} to Fe^{3+} using a UV-vis spectrophotometer[2,3]:

$$Fe^{2+} + H_2O_2 \rightarrow Fe^{3+} + OH^- \qquad (1)$$

1 M KOH solutions containing different concentrations (45.7-482.3 μmol/L) of H_2O_2 was prepared. 2 mL of the above solutions were mixed with 1.8 mL HCl (3 M) and 0.4 mL FeSO4 (0.1 M) and stirred for 2 min. Then the absorption spectra of the solutions were measured with a UV-vis spectrophotometer (Shimadzu UV-2600). The calibration equation was obtained by linearly fitting the peak intensity of the UV-vis spectra at 330 nm versus the H_2O_2 concentrations (Figure S1):

$$y = 6.2 + 481.8x \qquad (2)$$

where x is the intensity of the absorption peak at 330 nm and y is the H_2O_2 concentration.

Electrochemical measurements of the CC/CMK-3 cathode. The electrochemical properties of the CC/CMK-3 cathode for O_2 reduction reaction were measured using a potentiostat (BioLogic SP-200) in a three-electrode configuration. CC/CMK-3 cathode (1 × 1 cm^2 in size), Pt wire, and Hg/HgO electrode were used as the working electrode, counter electrode, and reference electrode, respectively. 1 M KOH (pH 13.6) was used as the electrolyte and the temperature of the electrolyte was maintained at 283 K using

a constant temperature water circulator. During the electrochemical measurements, the electrolyte was magnetically stirred and the air was blown to the surface of the CC/CMK-3 cathode using a circulation pump. Linear scanning voltammograms (current-potential curves) were recorded in a cathodic scan at a rate of 10 mV/s. The potential measured versus the Hg/HgO reference electrode ($E_{Hg/HgO}$) was converted to the RHE scale (E_{RHE}) according to the Nernst equation,

$$E_{RHE} = E_{Hg/HgO} + 0.0582 \times pH + 0.098 \quad (3)$$

Chronoamperometry curves were measured at an applied potential of 0.65 V versus RHE. During the chronoamperometry tests, 2 mL of the electrolyte was taken every 20 min, mixed with 1.8 mL HCl (3 M) and 0.4 mL $FeSO_4$ (0.1 M), and stirred for 2 min. The absorption spectra of the mixed solutions were then measured with a UV-vis spectrophotometer (Shimadzu UV-2600). The H_2O_2 concentrations were then calculated using the calibration equation (Eqn. 2). The Faradaic efficiency was calculated according to the following equation:

$$FE\ (\%) = \frac{V \cdot n}{\frac{Q}{2e^-} \times \frac{1}{N_A}} \times 100\% \quad (4)$$

where FE is the Faradaic efficiency; V is the volume of the solution, in L; n is the H_2O_2 concentration in the solution, in μmol/L; Q is the total charge passed, in C; e^- is the electron charge, $1.602 \times 10^{-19}\ C$; N_A is Avogadro's constant, 6.02×10^{23}.

Bias-free H_2O_2 production properties of the Mg:Ta_3N_5||Nafion||CC/CMK-3 device. The bias-free photoelectrochemical H_2O_2 production using the Mg:Ta_3N_5/NiCoFe-B_i photoanode and the CC/CMK-3 cathode was conducted in a tailor-made cell equipped with gas/electrolyte inlets/outlets and a quartz window (Figures 3 & S6). The photoanode and cathode chambers were separated using a Nafion 117 membrane. The anolyte (1 M KOH, pH 13.6) was circulated in the photoanode chamber using a circulation pump. The catholyte (1 M KOH, pH 13.6) and air were circulated in the

cathode chamber using two separate circulation pumps. The temperature of both the anolyte and catholyte was maintained at 283 K using a water chiller. CC/CMK-3 cathode with a size of 5 × 5 cm^2 was used and the active area of the Mg:Ta_3N_5/NiCoFe-B_i photoanode was approximately 0.95 cm^2. Photoelectrochemical H_2O_2 production properties of the assembled Mg:Ta_3N_5||Nafion||CC/CMK-3 devices were tested using a potentiostat (BioLogic SP-200) in a two-electrode configuration. The H_2O_2 concentration in the electrolyte was measured every 20 min during the reaction using the Fe^{2+} colorimetric method. The solar-to-fuel conversion efficiency (STF) was calculated from the amount of H_2O_2 produced under simulated or natural sunlight,

$$STF(\%) = \frac{\Delta G_{H_2O_2} \times n_{H_2O_2}}{t_{ir} \times S_{ir} \times I_{AM}} \times 100\% \quad (5)$$

where $\Delta G_{H_2O_2}$ is the Gibbs free energy of H_2O_2 generation, 117 KJ/mol; $n_{H_2O_2}$ is the amount of H_2O_2 produced (mol); t_{ir} and S_{ir} represent irradiation time (s) and irradiated area (m^2), respectively; I_{AM} is irradiation intensity, which equals to $1000\ W/m^2$ for AM 1.5G simulated sunlight. The natural sunlight intensity during the outdoor test was monitored using a certified reference cell (Konica-Minolta AK-200).

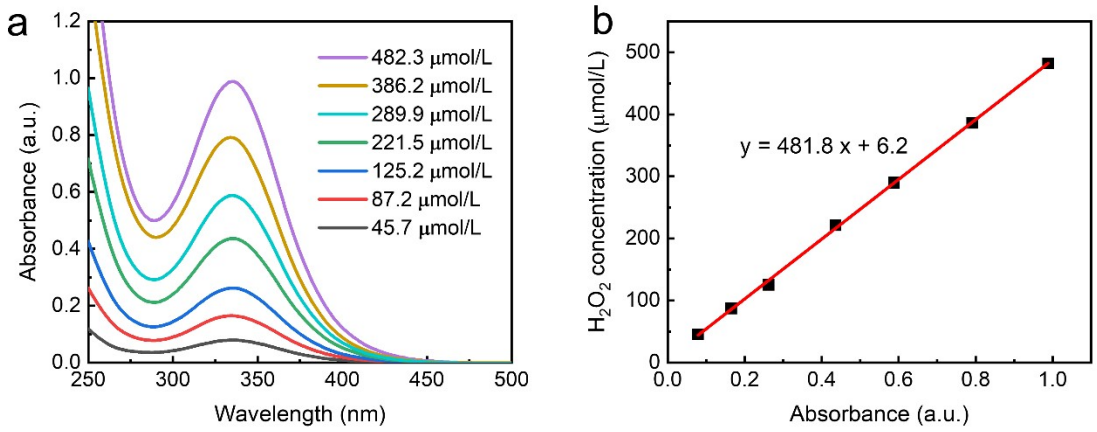

Figure S1. (a) UV-vis absorption spectra of 1 M KOH electrolyte with H_2O_2 different concentrations using the Fe^{2+} colorimetric method. (b) Calibration curve of the H_2O_2 concentration in 1 M KOH electrolyte**.** Inset shows the calibration equation for determining the H_2O_2 concentration.

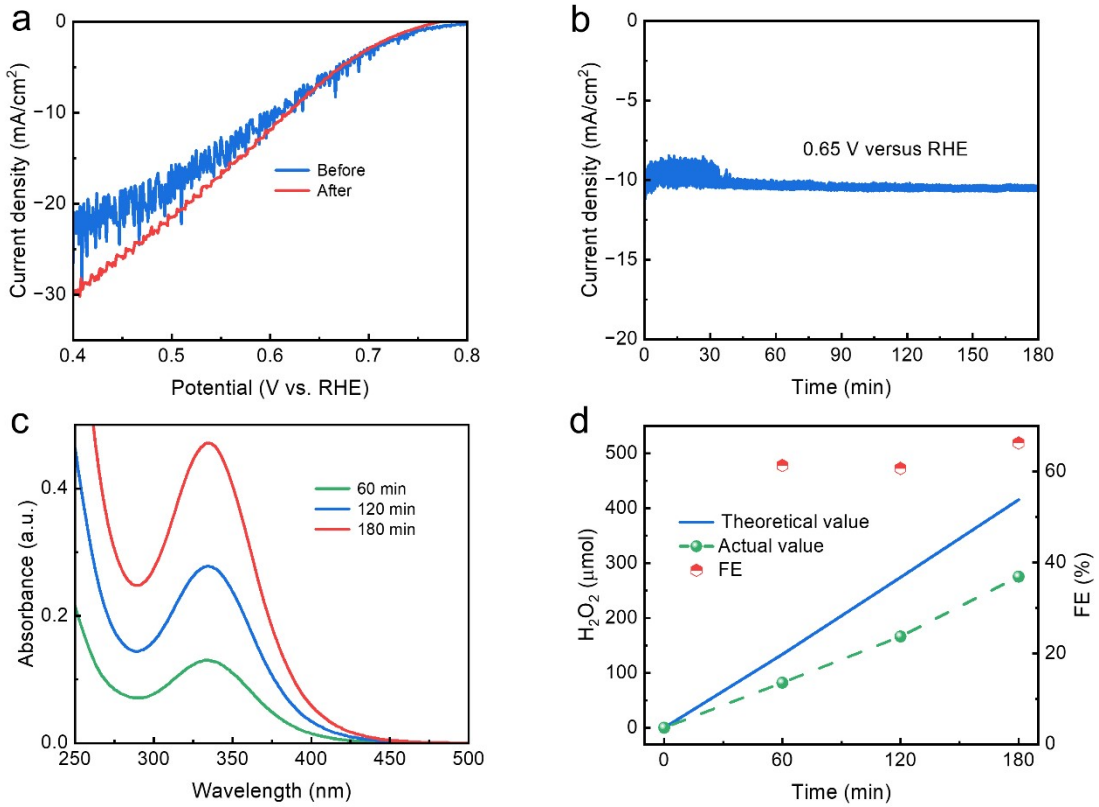

Figure S2. (a) J-V curves of the carbon paper (CP) loaded with 0.085 mg/cm^2 CMK-3 catalyst measured in 1 M KOH electrolyte at 283 K before and after the stability test. (b) Steady-state current measured at 0.65 V vs. RHE in 1 M KOH electrolyte at 283 K. (c) UV-vis absorption spectra of the electrolyte at different times during the stability test using the Fe^{2+} colorimetric method. (d) Amount of H_2O_2 produced and the calculated Faradaic efficiency (FE) of the CP/CMK-3 cathode.

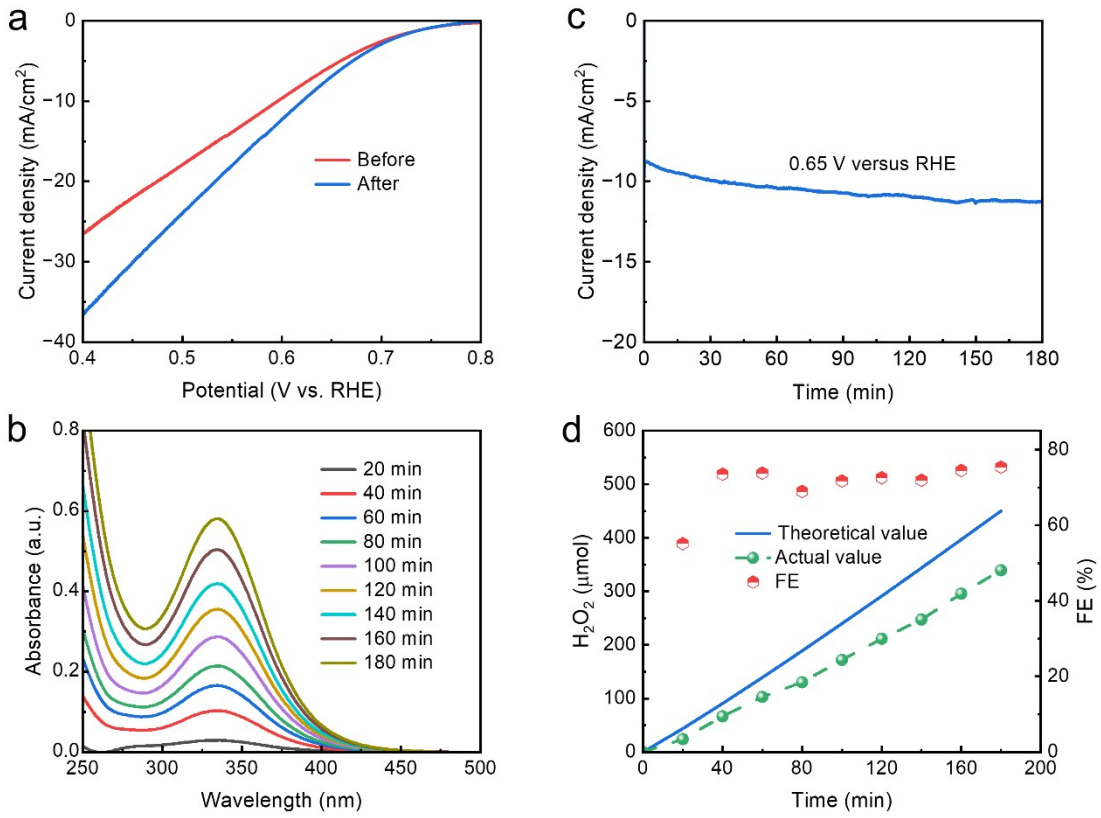

Figure S3. (a) J-V curves of the carbon cloth (CC) loaded with 0.05 mg/cm^2 CMK-3 catalyst measured in 1 M KOH electrolyte at 283 K before and after the stability test. (b) Steady-state current measured at 0.65 V vs. RHE in 1 M KOH electrolyte at 283 K. (c) UV-vis absorption spectra of the electrolyte at different times during the stability test using the Fe^{2+} colorimetric method. (d) Amount of H_2O_2 produced and the calculated Faradaic efficiency (FE) of the CC/CMK-3 cathode.

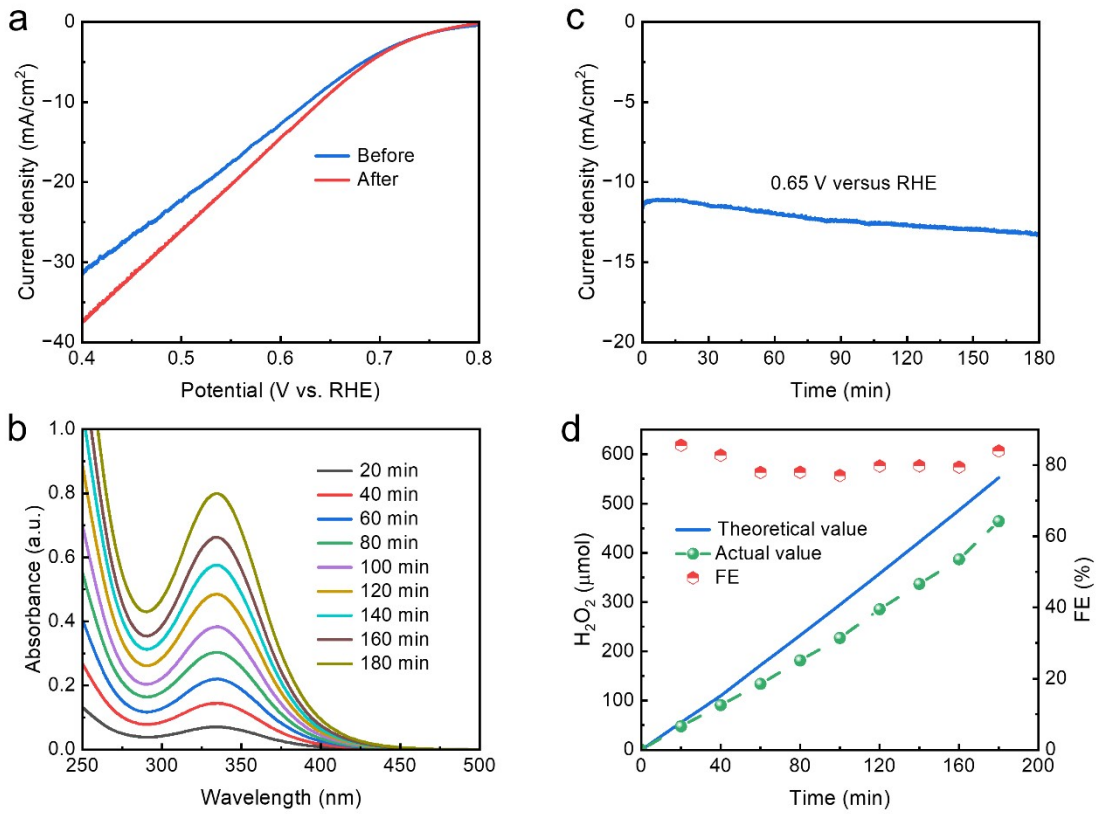

Figure S4. (a) J-V curves of the carbon cloth (CC) loaded with 0.11 mg/cm^2 CMK-3 catalyst measured in 1 M KOH electrolyte at 283 K before and after the stability test. (b) Steady-state current measured at 0.65 V vs. RHE in 1 M KOH electrolyte at 283 K. (c) UV-vis absorption spectra of the electrolyte at different times during the stability test using the Fe^{2+} colorimetric method. (d) Amount of H_2O_2 produced and the calculated Faradaic efficiency (FE) of the CC/CMK-3 cathode.

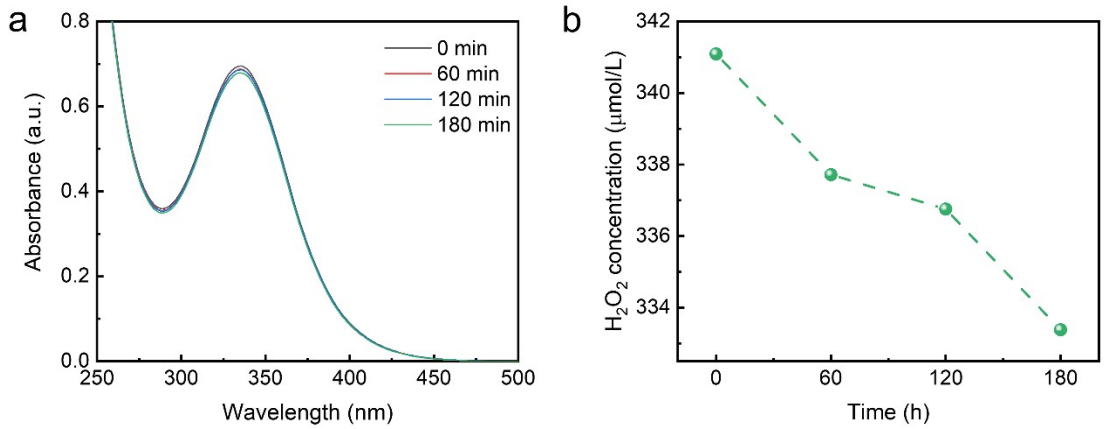

Figure S5. Self-decomposition of H_2O_2 in KOH electrolyte at 283 K. (a) UV-vis absorption spectra of the electrolyte measured every 60 min using the Fe^{2+} colorimetric method. (b) Change of H_2O_2 concentration with time.

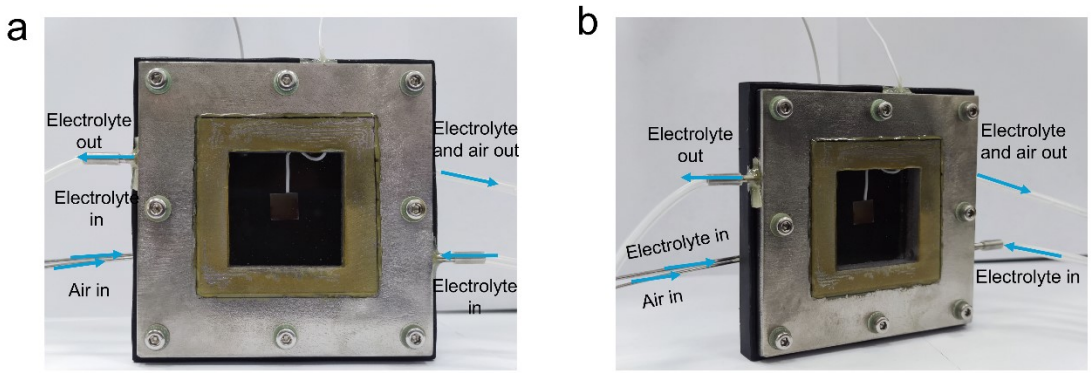

Figure S6. Photographs of the assembled Mg:Ta_3N_5||Nafion||CP/CMK-3 device.

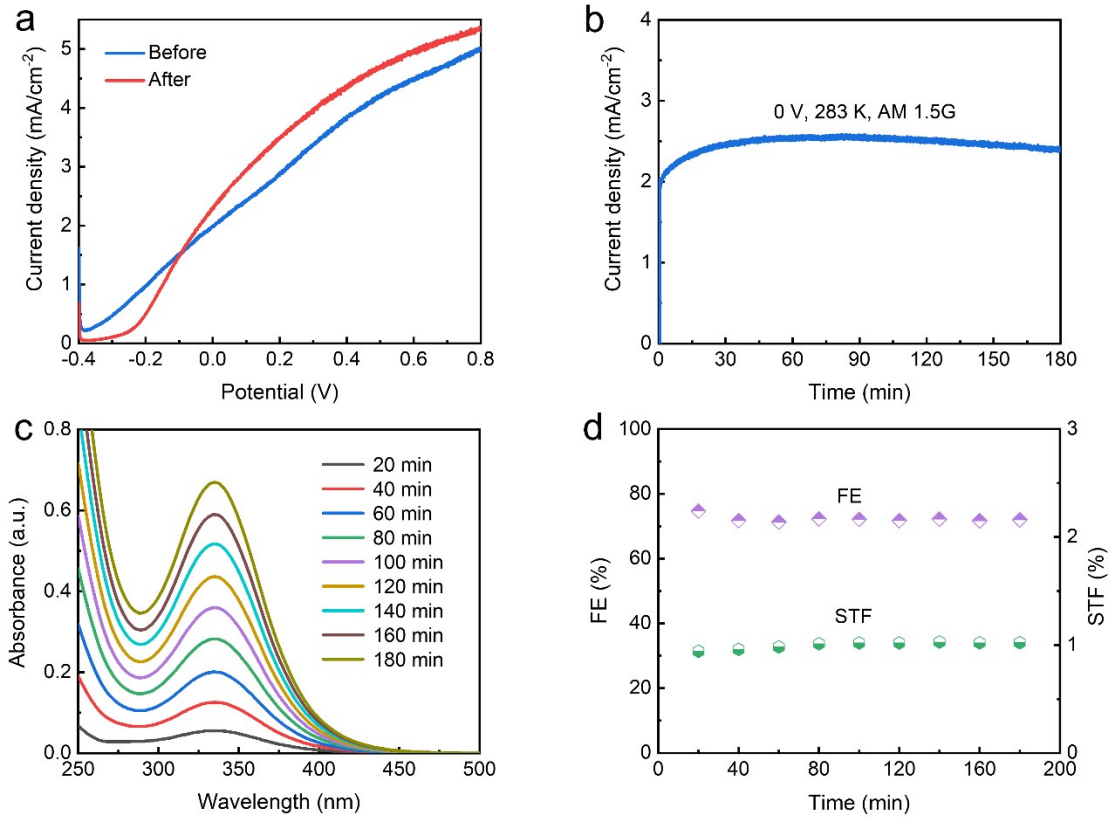

Fig. S7. (a) J-V curves of the Ta_3N_5||Nafion||CC/CMK-3 device measured in 1 M KOH electrolyte at 283 K before and after the stability test under AM1.5G simulated sunlight. Undoped Ta_3N_5 modified with NiCoFe-B_i co-catalyst was used as the photoanode. (b) Photocurrent of the Ta_3N_5||Nafion||CC/CMK-3 device measured at zero bias in 1 M KOH electrolyte at 283 K under AM1.5G simulated sunlight. (c) UV-vis absorption spectra of the electrolyte measured every 20 min during the stability test using the Fe^{2+} colorimetric method. (d) FE and STF of the Ta_3N_5||Nafion||CC/CMK-3 device.

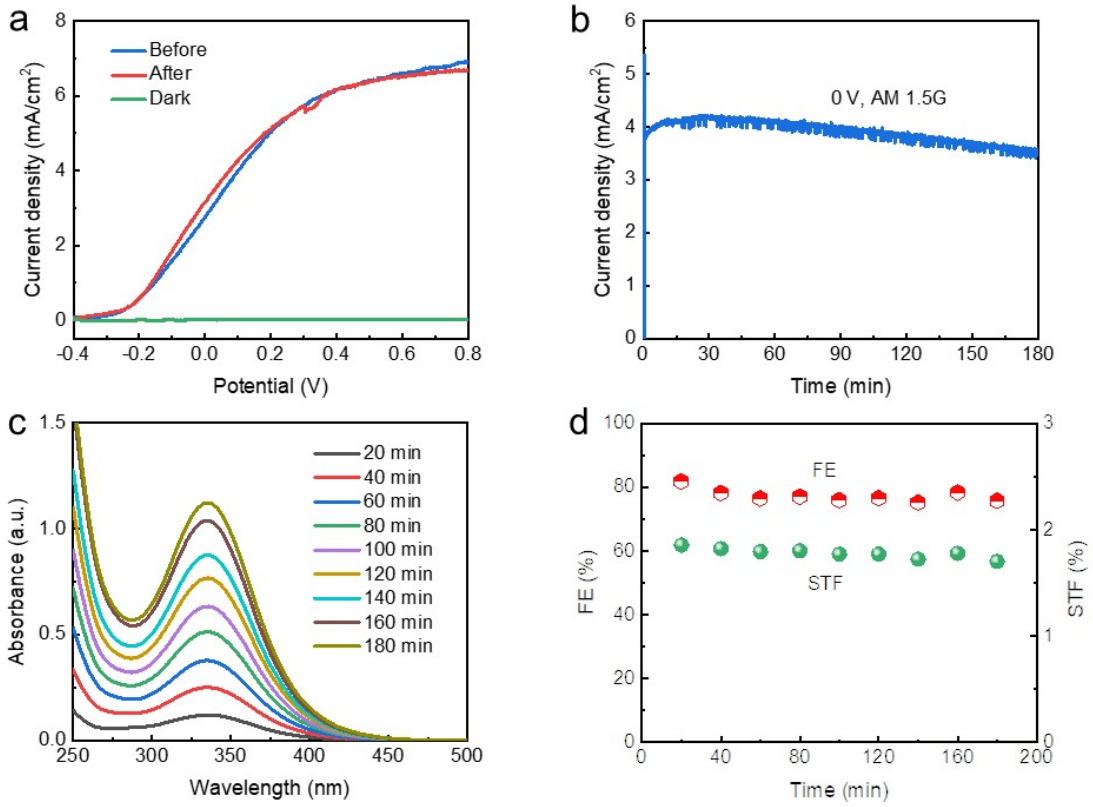

Fig. S8. (a) J-V curves of the Mg:Ta_3N_5||CC/CMK-3 device without a Nafion membrane measured in 1 M KOH electrolyte at 283 K before and after the stability test under AM1.5G simulated sunlight and in the dark. (b) Photocurrent of the Mg:Ta_3N_5||CC/CMK-3 device measured at zero bias in 1 M KOH electrolyte at 283 K under AM1.5G simulated sunlight. (c) UV-vis absorption spectra of the electrolyte measured every 20 min during the stability test using the Fe^{2+} colorimetric method. (d) FE and STF of the Mg:Ta_3N_5||CC/CMK-3 device.

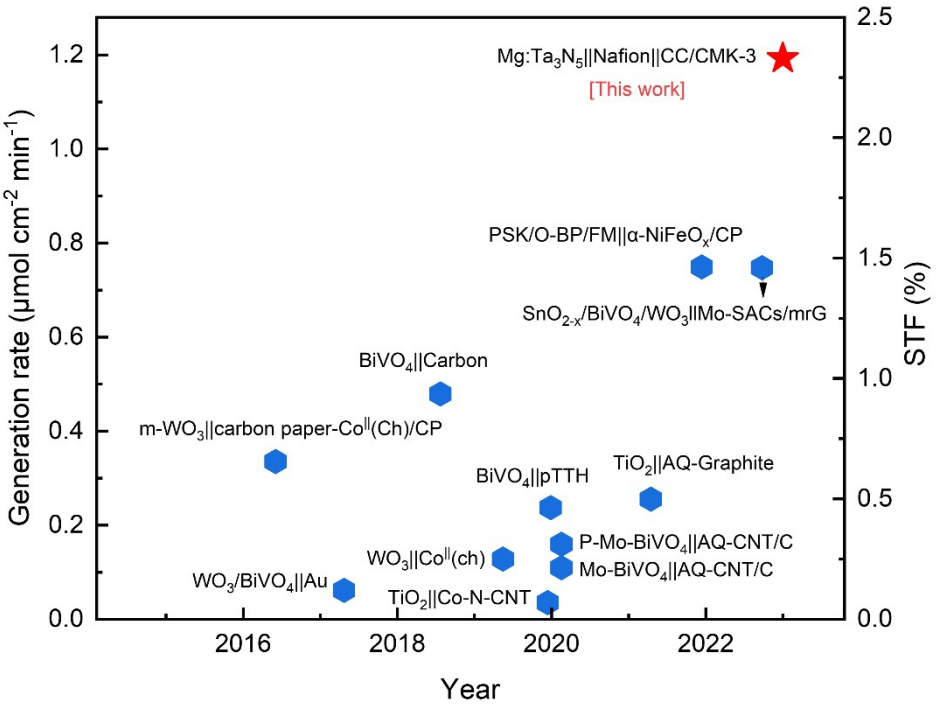

Fig. S9. Summary of the performance of the PEC devices for bias-free H_2O_2 production. The left and right axes show the H_2O_2 production rate and the corresponding STF of the devices, respectively. More details are provided in Table S1.

Table S1. Comparison of recent-reported bias-free PEC systems for the production of H_2O_2. (OER: oxygen evolution reaction, ORR: oxygen reduction reaction to form H_2O_2, WOR: water oxidation reaction to form H_2O_2)

System components (anode||cathode)	Generation rate (μmol*cm^{-2}*min^{-1})	STF (%)	Anode reaction	Cathode reaction	Year	Ref.
m-WO_3||CP/Co^{II} (Ch)	0.28	0.55	OER	ORR	2016	4
WO_3/$BiVO_4$||Au	0.0614	0.12	OER	ORR	2016	5
$BiVO_4$||carbon	0.48	0.94	WOR	OER	2018	6
TiO_2||Co-N-CNT	0.035	0.069	OER	ORR	2019	7
WO_3||Co^{II} (ch)	0.13	0.25	OER	ORR	2019	8
$BiVO_4$||pTTH	0.238	0.46	OER	ORR	2020	9
P-Mo-$BiVO_4$||AQ-CNT/C	0.16	0.31	WOR	OER	2020	10
TiO_2||AQ-Graphite	0.26	0.5	OER	ORR	2021	11
PSK/O-BP/FM ||α-$NiFeO_x$/CP	0.66	1.46	OER	ORR	2021	12
SnO_{2-x}/$BiVO_4$/ WO_3||Mo-SACs/ mrG	0.76	1.463	WOR	ORR	2022	13
Mg:Ta_3N_5||Nafion| |CC/CMK-3	1.19	2.33	OER	ORR	2023	This work

Supplementary References

1. Y. Xiao, C. Feng, J. Fu, F. Wang, C. Li, V. F. Kunzelmann, C.-M. Jiang, M. Nakabayashi, N. Shibata, I. D. Sharp, K. Domen and Y. Li, *Nat. Catal.*, 2020, **3**, 932-940.
2. K. Fuku, Y. Miyase, Y. Miseki, T. Gunji and K. Sayama, *ChemistrySelect*, 2016, **1**, 5721-5726.
3. K. Fuku and K. Sayama , *Chem. Commun*., 2016, **52** , 5406.
4. K. Mase, M. Yoneda, Y. Yamada and S. Fukuzumi, *Nat. Commun.*, 2016, **7**, 11470.
5. K. Fuku, Y. Miyase, Y. Miseki, T. Funaki, T. Gunji and K. Sayama, *Chem. Asian J.*, 2017, **12**, 1111-1119.
6. X. Shi, Y. Zhang, S. Siahrostami and X. Zheng, *Adv. Energy Mater.*, 2018, **8**, 1801158.
7. M. Ko, L. T. M. Pham, Y. J. Sa, J. Woo, T. V. T. Nguyen, J. H. Kim, D. Oh, P. Sharma, J. Ryu, T. J. Shin, S. H. Joo, Y. H. Kim and J. W. Jang, *Nat. Commun.*, 2019, **10**, 5123.
8. J. Liu, Y. Zou, B. Jin, K. Zhang and J. H. Park, *ACS Energy Lett.*, 2019, **4**, 3018-3027.
9. W. Fan, B. Zhang, X. Wang, W. Ma, D. Li, Z. Wang, M. Dupuis, J. Shi, S. Liao and C. Li, *Energy Environ. Sci.*, 2020, **13**, 238-245.
10. T. H. Jeon, H. Kim, H.-i. Kim and W. Choi, *Energy Environ. Sci.*, 2020, **13**, 1730-1742.
11. T. H. Jeon, B. Kim, C. Kim, C. Xia, H. Wang, P. J. J. Alvarez and W. Choi, *Energy Environ. Sci.*, 2021, **14**, 3110-3119.
12. C. Dong, Y. Yang, X. Hu, Y. Cho, G. Jang, Y. Ao, L. Wang, J. Shen, J. H. Park and K. Zhang, *Nat. Commun.*, 2022, **13**, 4982.
13. R. Mehrotra, D. Oh and J. W. Jang, *Nat. Commun.*, 2021, **12**, 6644.